International Conference on Control, Engineering & Information Technology (CEIT'14)
Proceedings - Copyright IPCO-2014, pp. 159-164
ISSN 2356-5608

Verification of a Pyroelectric Sensor Model using Measurements and an Optimization Algorithm

Nejmeddine Sifi[1], Oualid Touayar[2]

University of Carthage, National Institute of Applied Sciences and Technology,
Research Laboratory « Materials, Measurements and Applications »,
INSAT, Département de Génie Physique et Instrumentation, BP 676, 1080 Tunis Cedex, Tunisia
[1]nejm.sifi@fss.rnu.tn
[2]touayar.walid@planet.tn

***Abstract* — The objective of this paper is twofold. On the one hand showing that an equivalent electrical model can account appropriately and at the behavioural level, the physical phenomena involved in an electronic device; this is achieved by comparing the simulated response of the model with a measured response resulting from an actual prototype of the device under test. On the other hand, demonstrating the reliability of an optimization algorithm to estimate the parameters values of an equivalent electrical model using a succession of tests and adjustments so that the algorithm converges to and reaches the optimal solution. The optimization algorithm is a combination of two search methods: random and deterministic. In this paper, the optimization algorithm is described and results obtained from its application to a pyroelectric sensor equivalent electrical circuit model are presented and discussed.**

***Keywords* — Modeling; Parameters estimation; Optimization algorithm; Pyroelectric sensor; Measurement.**

I. INTRODUCTION

Modeling and simulation becomes more and more important in different areas of the electronics industry. The accuracy of simulation results depends on the electronic devices models and their parameters. Therefore, the modeling of devices and the estimation of their parameters values is always one of the most important research directions in electronic technology. Furthermore, the reliability of electronic circuit design simulators depends substantially on the validity of the models which are implemented in the simulators and on the knowledge of the parameters which appear in the models.

Different categories of devices models are studied and used but it is commonly known that "behavioral" or "empirical" models are simple and easy-to-use even if they present less accuracy [1]–[6]. This class of models is based on electrical equivalent circuits. Moreover, after the initial design phase of the equivalent model, the second phase is to determine the best values of the parameters constituting the model. This is achieved by using an appropriate method for this purpose. A semi-experimental approach to achieve this goal is by fitting the measured data obtained from a prototype device as closely as possible to the simulated data. The main component of this approach is an optimization algorithm.

Optimization of equivalent electrical models in time domain using measurements is more and more used for solving different problems. However, it is well known that in an optimization algorithm for a realistic device, the objective function to be optimized usually combines conflicting goals [7], [8]. Therefore, it may have several local minima even very different from the global one. The purpose of this paper is to show how good results can be obtained when optimizing equivalent electrical models by combining two different algorithms and using time domain measurements. The chosen application case is an electrical equivalent model of pyroelectric sensors proposed by Cornelius et al. [9].

II. OPTIMIZATION ALGORITHM

The principle of the method is described in Fig. 1. The first step is the design of an equivalent model of the device. The second step is simulation and optimization. For this, we use an electrical simulator for general purposes (SPICE like simulator). This simulator has been associated with an optimization algorithm specially developed and adapted to the problems of fitting parameters of equivalent electrical models (choice of the objective function, sensitivity to different parameters ... etc.).

The study performed was relevant to find out the best way of coupling two different optimization algorithms in order to obtain the best results in detecting the optimal variables set inside the feasibility area (i.e. the initial area limits). The first algorithm used is based upon a random procedure. It has the ability to avoid to be trapped in local minima. The second one is a conjugate-gradient algorithm (the Steepest Descent) which completes the optimization when the global optimum zone is detected. For the two algorithms, an objective function is used. This function estimates numerically the correlation between the simulated response of the equivalent electrical model and measurement.

The objective function chosen for our application is defined as follows [10]

$$\text{Objective function } \rho = \frac{\sigma_{xy}}{\sigma_x . \sigma_y} = \frac{\frac{1}{N}\sum_{i=1}^{N}(x_i - \bar{x})(y_i - \bar{y})}{\sqrt{\frac{1}{N}\sum_{i=1}^{N}(x_i - \bar{x})^2}\cdot\sqrt{\frac{1}{N}\sum_{i=1}^{N}(y_i - \bar{y})^2}} \quad (1)$$

International Conference on Control, Engineering & Information Technology (CEIT'14)
Proceedings - Copyright IPCO-2014, pp. 159-164
ISSN 2356-5608

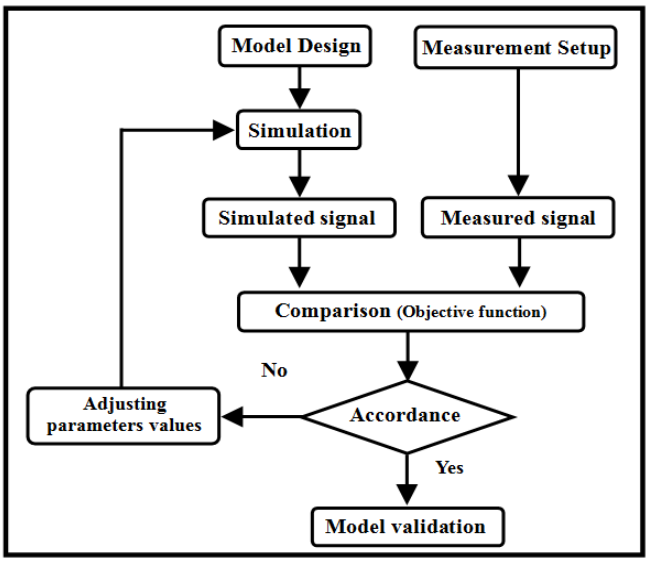

Fig. 1. Model parameters estimation methodology.

where x_i and y_i are the measured and the simulated data respectively, N is the maximum number of discrete data chosen for comparison, σ_{xy} is the covariance of the two signals, σ_x and σ_y are the standard deviations of the measured and simulated signals respectively. The random search algorithm is used as a first step in the search for an optimal solution. It is a preliminary procedure to locate a possible optimal area within the feasibility space. During this step, the values of the model parameters are obtained by a random selection within the values space initially fixed. Indeed, the user selects one of the statistical laws proposed by the algorithm (normal distribution, uniform distribution ... etc.) and the values of the parameters are randomly generated and tested. This way of obtaining the values of the model parameters allows the algorithm to avoid to be trapped in local minima. As second step we used the so-called "steepest descent" method [11]. This is a classic method that uses the gradient of an objective function to evaluate the direction that the search must take, inside the optimal zone, to reach the global optimum point. At each iteration, the derivatives of an objective function $F(\alpha)$ are calculated, where α is the set of designable parameters whose values may be modified during the optimization process. The primary reason for the use of derivatives is that at any point in the feasibility area, the negative gradient direction indicates the direction of the greatest rate of decrease of the objective function at this point. Furthermore, the numerical evaluation of the objective function derivatives is performed using a sensitivity analysis. The latter determines the numerical derivatives with the greatest possible precision. In "steepest descent" method, starting from an initial trial point α_l, iterative moves towards the optimum point are accomplished according to the rule

$$\alpha_{i+1} = \alpha_i + \beta_i.p_i \qquad (2)$$

where

$$p_i = -\nabla F(\alpha)\big|_{\alpha_i} \Big/ \left\| \nabla F(\alpha)\big|_{\alpha_i} \right\| \qquad (3)$$

i.e., p_i is given by the negative of the normalized gradient vector at the present value of α at the i^{th} iteration. The function ∇F is defined as

$$[\partial F/\partial\alpha_1, \partial F/\partial\alpha_2, ..., \partial F/\partial\alpha_k]^t \qquad (4)$$

The step length β_i is obtained from an one-dimensional search along the pi direction. However, as for other gradient methods, its main drawback is related to its dependence on the starting point. For this reason, the "steepest descent" seems to be well-suited as second step algorithm to locate the optimum parameters starting from the values found with a "random search".

III. Electrical Equivalent Model of a Pyroelectric Sensor

A. Theoretical overview

The evolution of the physical phenomena inside the sensor is as described by Hamilton et al. [12]. Fig. 2 shows a cross-sectional representation of a typical pyroelectric sensor. The incident optical radiation generates heat in the absorption layer on the surface of the sensor. Furthermore, the metallic electrode is used for electric heating; this optional operation is used for calibration applications. The second metallic electrode is used for the recovery of the electric signal in the form of an electrical short-circuit current $I_P(t)$. This current is measured using a current-voltage converter. A substrate layer is often used to provide mechanical stability and acts as a heat sink to change the frequency response of the sensor.

1) Determination of the current response

The determination of the current response $I_P(t)$ obtained from a pyroelectric sensor can be made based on the expressions established by Mopsik and DeReggi [13]. So if only the polarization $P(x)$, expressed in terms of the depth x, is considered, it is shown that the current $I_P(t)$, measured per unit area of the sensor as a function of time t, is given by [9]

$$I_P(t) = (C_1 + C_2)\int_0^d P(x)\frac{d\theta(x,t)}{dt}dx - \frac{C_2}{d}\int_0^d P(x)dx\int_0^d \frac{d\theta(x,t)}{dt}dx \qquad (5)$$

where $C_1 = \lambda_p/d$ and $C_2 = (\lambda_x - \lambda_\varepsilon)/d$.

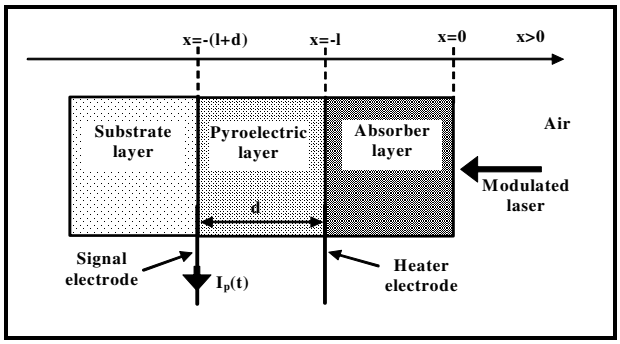

Fig. 2. Cross-sectional representation of a pyroelectric sensor.

International Conference on Control, Engineering & Information Technology (CEIT'14)
Proceedings - Copyright IPCO-2014, pp. 159-164
ISSN 2356-5608

λ_x, λ_ε and λ_p are the coefficient of thermal expansion and the temperature coefficients of dielectric constant and permanent polarization respectively, d is the thickness of the pyroelectric, and $\theta(x,t)$ is the temperature of the pyroelectric at x and t. For convenience, $I_P(t)$ and P(x) are normalized with respect to the mean polarization so that

$$P'(x) = d.P(x)\int_0^d P(x)dx \tag{6}$$

and

$$I'_P(t) = d.I_P(t)\int_0^d P(x)dx = \int_0^d G(x)\frac{d\theta}{dt}dx \tag{7}$$

where

$$G(x) = (C_1 + C_2)\,P'(x) - C_2 \tag{8}$$

In this manner, the waveform of $I_P(t)$ is preserved in $I_P'(t)$.

2) Determination of the electrical equivalent model

The determination of an equivalent electrical model of a pyroelectric sensor is based on some justified simplifying assumptions. First, it is assumed that the heat flow through the sensor is one-dimensional. This is justified by the large planar dimensions of heat sources compared to the thickness of the materials used. Then, each of the constituent layers of the pyroelectric sensor is characterized by a thermal resistance R_{th} and a thermal capacity C_{th}. R_{th} and C_{th} are determined by the thermal properties of the material and the width of the layer.

The equivalent electrical model of the pyroelectric sensor is then established by using an electrical resistance R_e and an electrical capacitance C_e representing R_{th} and C_{th} respectively [9], [14]. Furthermore, a thermal time constant τ_{th} for a layer of material is defined as follows

$$\tau_{th} = R_{th}C_{th} \tag{9}$$

This thermal time constant is also related to the physical characteristics of the material such as

$$\tau_{th} = R_{th}.C_{th} = (d/h)(\rho g d) \tag{10}$$

where d is the thickness of the layer, ρ is the density of the material, g is the specific heat, and h is the thermal conductivity of the material. Similarly, the electrical equivalent of a layer has a time constant τ_e given by

$$\tau_e = R_eC_e \tag{11}$$

It should be noted that for modeling purposes, a discrete element approximation is made. The propagation of the heat wave is imagined occurring through a succession of discrete elementary cells, *i.e.*, the pyroelectric sensor is imagined to be cut, parallel to the surface, into a number of consecutive slices. If a layer of material is represented by N separate slices, then the width of each slice is N^{-1} of the total width of the layer. The thermal capacitance and thermal resistance can be treated similarly. Finally, the continuous integral of Eq. (7) is replaced by the discrete element summation approximation

$$I'_P(t) \cong \sum_{i=1}^{N} G_i \frac{d\theta_i(t)}{dt} \tag{12}$$

B. Equivalent circuit design

The phenomenon of the heat wave propagation in the sensor and the creation of an output current are represented by the equivalent circuit model of Fig. 3 [9].

The output signal obtained from the equivalent circuit is proportional to $I'_P(t)$ as defined by Eq. (12). The equivalent circuit model is constituted by a network of resistors and capacitors. The absorber layer is represented by a resistor-capacitor combination (R_a, C_a) suitably arranged. This part of the model has as an input, a pulse voltage source with a total power contained in each pulse equivalent to that contained in each optical pulse from the actual laser source. The substrate layer is also composed of a resistor-capacitor combination (R_s, C_s) properly arranged. Pyroelectric layer is represented by a succession of cells (R_p, C_p) modeling each of the sub-layers resulting from the virtual division of the pyroelectric layer.

The number of cells (R_p, C_p) is dependent on the smoothness of simulation that the user wishes. A compromise must be accepted because as the number of cells is important as the smoothness of simulated signal is much better and the overall simulation time is important. The voltage at the node between the resistances R_p is equivalent to the temperature θ_i in the discrete element model and the corresponding current through a capacitor C_p is proportional to $d\theta_i/dt$. As the thermal resistance of the metallic electrode layers is insignificant, these layers are represented by single capacitors.

IV. TIME DOMAIN MEASUREMENTS

In order to get an electrical signal, image of the variation of the sensor temperature, we measure the voltage at the output of a charge–current converter (Fig. 4) [15]. The obtained output voltage V_0 is independent from the capacity of the sensor and the connecting cables.

The variation of the pyroelectric current, $I_p(t)$, is given by Eq. (13).

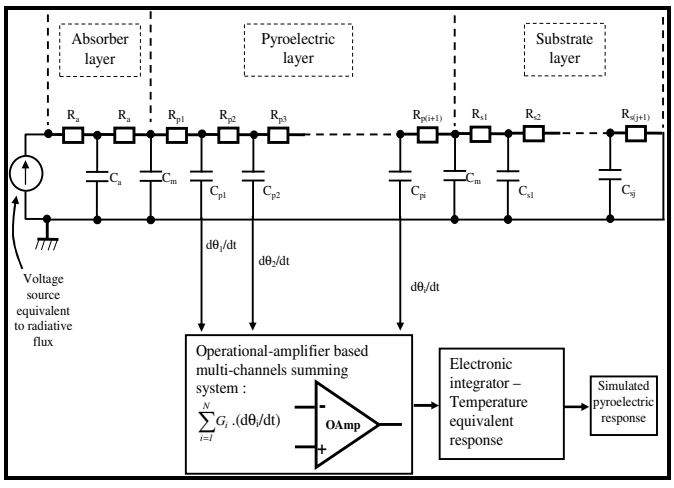

Fig. 3. Electrical equivalent model used for simulating the pyroelectric sensor response. R and C are the electrical resistance and the electrical capacitance respectively. Subscript a, m, p and s refer to absorber, metal electrode, pyroelectric and substrate materials, respectively.

$$I_p(t) = -\left[\frac{C_p}{G_n} + \frac{C_n}{G_n} + C_n\right].\frac{dV_0}{dt} - \left[\frac{1}{R_p} + \frac{1}{Z_d}\right].\frac{V_0}{G_n} \quad (13)$$

Where experimentally, C_n = (1nF, 10nF), C_p = 1nF, R_p = 10^{11} Ω, Z_d = 10^{12} Ω, G_n = 2x10^5. Z_d and G_n are the input impedance and the gain of the operational amplifier respectively. Taking into account the experimental values of the different components, the following equation is obtained

$$I_p(t) = -C_n \frac{dV_0}{dt} \quad (14)$$

where

$$V_0(t) = -\frac{\Lambda.S.\varepsilon.C_{th}^{-1}}{C_n}.\exp(-\frac{t}{\tau_{th}}).E \quad (15)$$

Λ is the pyroelectric coefficient, S is an one face surface of the pyroelectric material, ε is the absorption coefficient of the absorbing black layer and E is a measure of the energy contained in the laser pulse given by the maximum value of the response [15]–[16]. In these conditions, the response $V_0(t)$ is of exponential form decreasing according to time with respect to the thermal time constant τ_{th}.

The experimental setup used to determine the temperature response is described in Fig. 5. A laser system of "YAG" type delivers 3W as a maximum radiant power at a wavelength equal to 532 nm. The beam is then focused at the entrance of a mechanical chopper. The focal distance is set to 50 mm. The chopping frequency is variable from 5 Hz to 22 Hz; this frequency is also the repetition rate of the laser pulses. The appropriate frequency is fixed manually, via an input/output interface, after different tests so to make it possible the sensor to return to a thermal state of balance. In fact, the hole on the mechanical chopper disk permits to obtain a pulse width T of about 4.75 ms; this value is less than the thermal time constant of the pyroelectric sensor tested in this study.

A numerical oscilloscope records the experimental responses of the pyroelectric sensor on a computer by the means of a serial interface (RS232). A variable gain instrumentation amplifier is also used. The amplifier is an AD620 which input impedance is about 10^{12} Ω and the capacity C_n is equal to 1 nF. The tested sensor is made of the polyvinylidine fluoride (PVF_2) as a pyroelectric material. The experimental temperature response of the tested pyroelectric sensor to a laser pulse width T of about 4.75 ms, for a material thickness of 9 µm, is given in Fig. 6 (black curve). For this sensor, we used a capacitor C_n = 1 nF and an input mean power of about 250 mW.

V. Optimization and Simulation Results

The objective is to make a double-check: the suitability of the chosen model with the device under test and the reliability of the optimization process to converge and achieve optimal estimation of the model parameters values. The optimized model has to give an electrical signal the same as the one measured previously. To achieve these goals, we applied the optimization algorithm to the case study presented in *section 4*.

Moreover, it must be noted that the optimization process requires predefining the maximum number of iterations and the minimum of the objective function to impose to the random search algorithm in order to continue optimizing by using the deterministic search. For the latter, the same parameters (maximum number of iterations and the minimum value of the objective function) must also be defined.

A preliminary study was performed to have indicators on the control parameters of the optimization process. The results have shown that for the "random search", a number of iterations of about 3500 is sufficient to reach an objective function ρ of the order of 0.90000. For the second algorithm and from the set of values found by the random search for a given optimization sequence, the number of iterations was set to 1000 and the objective function ρ was set to 0.99999. Furthermore, to obtain results for a relevant statistical analysis, we performed 1000 optimization processes for the measurement case study. Moreover, with regard to the processing of the 1000 optimization sequences results obtained, we performed the calculation of the mean values ($\bar{x}$), the standard deviations (σ_x) and the ratios ($\sigma_x/\bar{x}$) expressed in percentage; where x represents the parameters R_a, C_a, R_p, C_p, C_m, C_s and R_s.

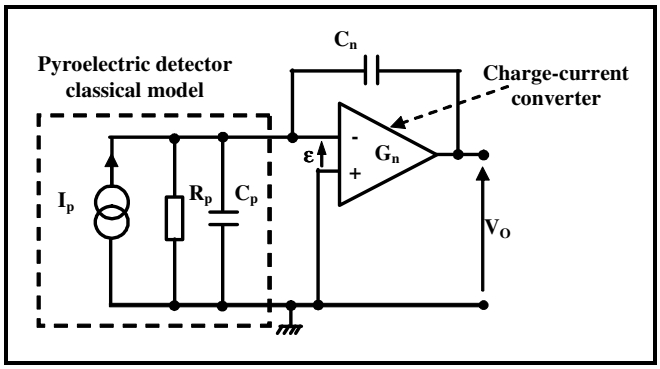

Fig. 4. Example of a charge – current converter circuit.

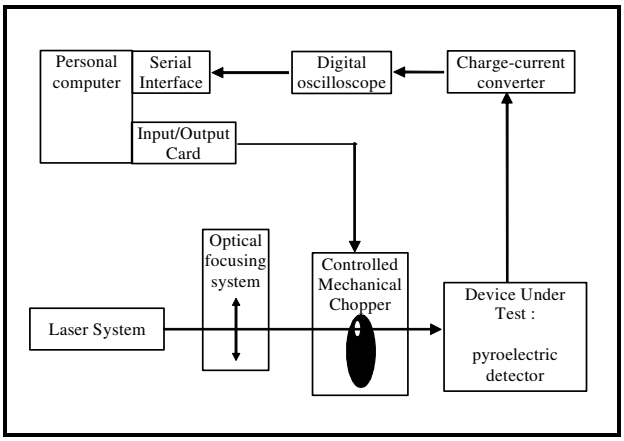

Fig. 5. Experimental setup used to measure the temperature equivalent signal of a pyroelectric sensor.

It should be noted that, given the number of optimization processes studied (equal to 1000), the distribution of the obtained results is statistically assumed to be a "Normal

Distribution" type, *i.e.,* a deviation of ±1σ around the mean value represents a space inside which the occurrence probability of the value called "true" is equal to 68%. A deviation of ±2σ is equivalent to 95% and ±3σ represents a probability of 99.7%. In addition, it is worth mentioning that the choice of the number of cells representing the layer of pyroelectric material is determined by the smoothness of the desired simulation. Indeed, always following the results of the preliminary study, a number of less than 10 cells did not allow obtaining an objective function "ρ" higher than 0.91732. The optimization process failed to converge to an optimal solution (i.e. failed to give an objective function ρ ≈ 0.99999). Indeed, the simulated signal tended to deviate extremely from the measured signal. Also, a number greater than 10 cells tended to increase the simulation time and do not significantly increase the correlation between the simulated and the measured signals. The analysis of the results obtained from the 1000 optimization sequences is summarized in Table I. In order to have more relevant evaluation indicators, we calculated the ratios $\sigma_x/\bar{x}$ expressed as a percentage (Table II). In addition, and in order to get a graphical idea of the model simulation result and compare it with the measured signal, we used the set of values that gave the highest objective function value; this set is called "best case" (Fig. 6). Thus, and from the overall results, the following comments can be formulated:

- The equivalent electrical model accounts appropriately for the behavior of the device under test, i.e., the pyroelectric sensor.
- The equivalent electrical model can be used to enrich the models library of any SPICE-like electrical simulation software for Computer Aided Design purposes.
- The combined optimization algorithm has shown its ability to determine an optimal solution (set of optimal values) to obtain a simulated response highly correlated with the measured signal.

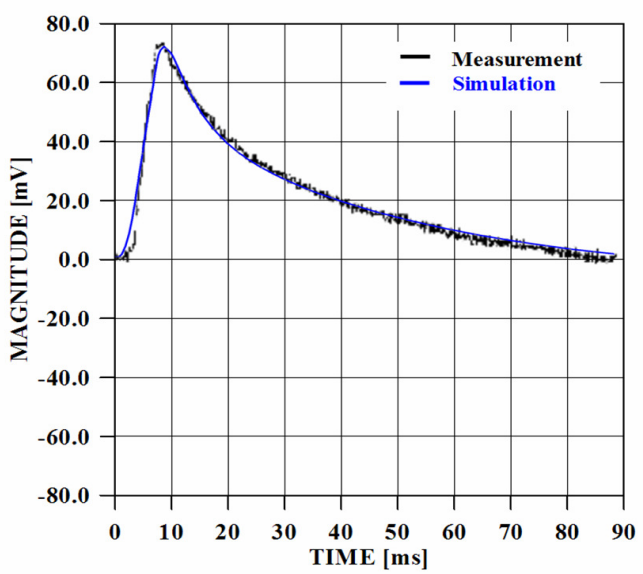

Fig. 6. Results obtained for the 9 µm thickness PVF_2 material sensor: a comparison between experimental and simulated waveforms.

TABLE I

NUMERICAL RESULTS OBTAINED FOR EACH PARAMETER OF THE SENSOR MODEL.

	Initial area limits Search		Optimization results				
	Min	Max	Mean value $\bar{x}$	Standard deviation at $1\sigma_x$	at $2\sigma_x$	at $3\sigma_x$	Best case Parameter
R_a [Ω]	1	500	11.337	0.133	0.266	0.399	11.471
C_a [µF]	0.01	20	1.254	0.015	0.030	0.045	1.236
R_p [MΩ]	1	100	7.286	0.127	0.254	0.381	7.139
C_p [pF]	1	1000000	682.624	8.123	16.246	24.492	696
C_m [nF]	1	1000000	13370.679	179.167	358.334	537.501	13185
R_s [Ω]	1	1000	2.702	0.973	1.946	2.919	9.648
C_s [pF]	1000	100000	3741.100	1173.658	2347.316	3520.974	9845
						Objective function ρ	**0.98732**

TABLE II

RATIOS $\sigma_x/\bar{x}$ CALCULATED FOR EACH PARAMETER OF THE MODEL USED AS INDICATORS OF OPTIMIZATION ALGORITHM PERFORMANCE.

Parameter	Mean value $\bar{x}$	$\pm1\sigma_x/\bar{x}$ [%]	$\pm2\sigma_x/\bar{x}$ [%]	$\pm3\sigma_x/\bar{x}$ [%]
R_a [Ω]	11.337	1.173	2.346	3.519
C_a [µF]	1.254	1.196	2.392	3.588
R_p [MΩ]	7.286	1.739	3.478	5.217
C_p [pF]	682.624	1.190	2.380	3.570
C_m [nF]	13370.679	1.340	2.680	4.020
R_s [Ω]	2.702	36.010	72.020	108.030
C_s [pF]	3741.100	31.372	62.744	94.116

Furthermore, the analysis of the calculated values $\sigma_x/\bar{x}$ [%] of the various parameters (R_a, C_a, R_p, C_p, C_m, C_s and R_s) shows the following:

- For parameters R_a, C_a, R_p, C_p and C_m, the results indicate that nearly at $\pm 1\sigma_x$ (i.e. 68% probability of existence of the "true value"), the dispersion of values obtained after 1000 optimization processes is 1.173%, 1.196%, 1.739%, 1.190% and 1.340% of the average values $\overline{R}_a$, $\overline{C}_a$, $\overline{R}_p$, $\overline{C}_p$ and $\overline{C}_m$ respectively. At near $\pm 2\sigma_x$ (i.e. 95% probability of existence of the true value), the dispersion of the values obtained is 2.346%, 2.392%, 3.478%, 2.380% and 2.680% of the average values $\overline{R}_a$, $\overline{C}_a$, $\overline{R}_p$, $\overline{C}_p$ and $\overline{C}_m$ respectively. These results are very encouraging and widely acceptable given the experimentally accepted tolerance levels. This also means that the set of optimal values is within the uncertainty region defined by $\pm 2\sigma_x$ with a probability of 95% and with a tolerance range from 2.346% to 3.478% (depending on parameters). These tolerances are practically very acceptable and the way to get them is consistent with methods of experimental data statistical analysis agreed to in the field of metrology.
- For parameters R_s and C_s: the results indicate tolerances to near $\pm 1\sigma_x$, 36.010% and 31.372% respectively and near $\pm 2\sigma_x$, 72.020% and 62.744% respectively. This indicates an almost complete insensitivity of the electrical equivalent model with respect to these parameters, and therefore the insensitivity of the mathematical function that goes with it as any part of an electrical circuit representing a physical effect is actually analyzed by any electrical simulator as a mathematical function. Although these elements represent physical phenomena, the results give the impression that the "substrate" layer has no effect on the behavioural pyroelectric sensor. A particular attention should be made to find the right solution to highlight this effect.

VI. Conclusion

A prospective study on models parameters estimation using time domain measurements and an optimization algorithm is presented. The combined optimization algorithm has been applied with success to a pyroelectric sensor electrical equivalent model and it has shown a very good ability to avoid to be trapped in local minima. The measurement used as an application example for the parameters values estimation was relevant to a PVF_2 sensor with 9 µm thickness. The results obtained were encouraging both in terms of the optimized parameters values and the reliability of the method. The whole semi-experimental modeling method can be applied to other types of sensors and the validated models can be included in the libraries of electrical simulators for computer aided design purposes.

Acknowledgment

The authors would like to thank Dr. I. Mellouki from the "Institut Préparatoire aux Etudes d'Ingénieurs de Tunis – Tunisia" for providing them with the measurements that were investigated.

References

[1] R. Al-Nazer, V. Cattin, P. Granjon, and M. Montaru, "A new optimization algorithm for a Li-Ion battery equivalent electrical circuit identification," in *Proc. 9th International Conference of Modeling, Optimization and Simulation (MOSIM 2012)*, June 06-08, 2012, Bordeaux, France.

[2] J. Chéron, M. Campovecchio, D. Barataud, T. Reveyrand, M. Stanislawiak, Ph. Eudeline, and D. Floriot, "Electrical modeling of packaged GaN HEMT dedicated to internal power matching in S-band," *International Journal of Microwave and Wireless Technologies*, vol. 5, pp. 495-503, 2012.

[3] E. Llobet, X. Vilanova, J. Brezmes, D. Lopez, and X. Correig, "Electrical equivalent models of semiconductor gas sensors using PSPICE," *Sensors and Actuators B*, vol. 77, pp. 275-280, 2001.

[4] P. Ramos, J. F. Meca, J. Mendiola, and E. Martin, "A Simple Thermal and Electrical Model of an Infrared Pyroelectric Detector using SPICE," in *Proc. Ferroelectrics, ISSN 0015-0193. IMF-10 International Meeting on Ferroelectricity*, vol. 10, Madrid, Spain, 2001.

[5] W. Y. Chung, T. P. Sun, Y. L. Chin, and Y. L. Kao, "Design of Pyroelectric IR Readout Circuit based on LiTaO3 Detectors," in *Proc. IEEE International Symposium on Circuits and Systems ISCAS'96*, vol. 4, pp 225-228, 1996.

[6] H. Vogt, "SPICE Modeling of Resistive, Diode and Pyroelectric Bolometer Cells," in *Proc. SPIE 6206 Infrared Technology and Applications XXXII*, 62061S, 2006.

[7] S. Koziel, and X. S. Yang, *Computational Optimization – Methods and Algorithms*, Series: Studies in Computational Intelligence. Springer vol. 356, pp. 284p, 2011.

[8] A. Antoniou, and W. S. Lu, *Practical Optimization – Algorithms and Engineering Applications*, Springer, vol. XIX, pp. 669, 2007.

[9] W. A. Cornelius, and R. V. Sargent, "Analog Technique for the Analysis of Pyroelectric Optical-Detection Signals," *Rev. Sci. Instrum.*, vol. 57(8), pp. 1574-1580, 1986.

[10] A. Ravindran, *Engineering Optimization - Methods and Applications*, Wiley, 2nd edition, 688p, 2006.

[11] J. M. Lewis, S. Lakshmivarahan, and S. Dhall, *Dynamic Data Assimilation – A least squares approach – Chapter 10 – Optimization – Steepest Descent Method*, Cambridge University Press, pp. 169-189, 2006.

[12] C. A. Hamilton, *An electrically calibrated pyroelectric radiometer system*, U.S. Dept. of Commerce, National Bureau of Standards, Institute for Basic Standards, Electromagnetics Division, 44p, 1976.

[13] A. Odon, "Voltage Response of Pyroelectric PVDF Detector to Pulse Source of Optical Radiation," *Measurement Science Review*, vol. **5**, Section 3, 2005.

[14] S. Efthymiou, and K. B. Ozanyan, "Pulsed Performance of Pyroelectric Detectors," *IOP Publishing Journal of Physics*, Conference Series, vol. 178, 012044, 2009.

[15] O. Touayar, N. Sifi, and J. Ben Brahim, "Theoretical and experimental study of power radiometric measurements using a pyroelectric current integrator converter," *Sensor and Actuators A – Physical*, vol. 135, pp. 484–491, 2007.

[16] O. Touayar, I. Mellouki, N. Sifi, and N. Yacoubi, "Determination of the nonequivalence radiative source between electrical and heating in a pyroelectric sensor using experimental voltage response and heating propagation theoretical model," *Sensor and Actuators A – Physical*, vol. 132, pp. 572–580, 2006.